J. Electrochem. Sci. Eng. **13(6)** (2023) 911-921; http://dx.doi.org/10.5599/jese.2032

Open Access : : ISSN 1847-9286
https://pub.iapchem.org/ojs/index.php/JESE

Original scientific paper

Synthesis, microstructure, and electrophysical properties of surface-modified polyantimonic acid nanoparticles

Fedor Yaroshenko[1,✉], Yulia Lupitskaya[1], Maxim Ulyanov[1,✉], Vladimir Burmistrov[1], Elena Filonenko[1], Damir Galimov[2], Danil Uchaev[2] and Ekaterina Rubtsova[1]

[1]*Chelyabinsk State University, 454001 Chelyabinsk, Russian Federation*
[2]*South Ural State University (National Research University), 454080 Chelyabinsk, Russian Federation*

Corresponding authors: ✉*fyaroshenko@yandex.ru*; ✉*max-39@yandex.ru*; Tel.: +7(351)799-71-19

Received: August 21, 2023; Accepted: September 23, 2023; Published: October 5, 2023

Abstract

This work has considered the modern ideas on the mechanism of surface modification for used nanodispersed inorganic modifiers with an acidic surface, which significantly affect the hydrate and transport properties of polymeric proton-conducting electrolytes. Authors have proposed an alternative approach consisting of the synthesis of new composite nanoscale systems characterized by high ionic conductivity and developed a method for obtaining composite materials with "core-shell" structure based on an inorganic proton conductor (polyantimonic acid) modified with silicon oxide. The surface morphology of the synthesized nanoparticles has been studied by transmission electron microscopy, and their sizes have been determined. The data on frequency dependence of the electrical impedance are presented and the behavior of the active and reactive components of the impedance and conductivity in the frequency range from 100 Hz to 1 MHz has been analyzed. An equivalent electrical circuit simulating the impedance dispersion for obtained composites with "core-shell" structure based on PAA and SiO_2 has been proposed.

Keywords

Nanoscale materials, core-shell particles, composite materials, impedance spectroscopy, proton conductivity

Introduction

The scientific and practical interest in the field of alternative energy to nanostructured materials and nanotechnologies lies in the potential to modify the surfaces of used nanoparticles and fundamentally change the properties of existing materials during the transition to the nanocrystalline state. Currently, active research aimed at enhancing the performance of polymer solid electrolytes commonly used in fuel cell technology [1-3]. One particular type of electrolyte, perfluorinated sulfonic cation exchange membranes like Nafion ("DuPont", USA) or the Russian

equivalent membrane MF-4SK ("Plastpolymer"), has exceptional properties including high proton conductivity, chemical and thermal stability, selectivity, and mechanical strength. However, the use of these membranes in various electrochemical devices has some limitations, notably a significant reduction in proton conductivity when operating under low humidity conditions [4].

One of the promising approaches aimed at improving the hydration and transport properties of Nafion-type polymers is their surface modification with nanodispersed particles of an inorganic proton conductor, which causes high ionic conductivity in the interfacial boundary layer of composites due to the enrichment of this layer with mobile charge carriers formed as a result of ion-exchange processes between the composite components.

It is known that using nanosized inorganic modifiers with an acidic surface has a significant effect on the transport properties of polymeric proton-conducting materials [5] and provides a number of advantages. It was shown in [6-11] that the grafting of acidic groups onto the surface of silicon oxide leads not only to an increase in the ionic conductivity of MF-4SK composite membranes but also contributes to their moisture content growth and ion-exchange capacity increase. Similar patterns in the conductive properties change of Nafion-type polymers were observed when they were doped with surface-modified particles of titanium oxide [12], zirconium [13], cerium [14], *etc*. [15-17]. In this regard, the choice of a modifying additive, such as polyantimonic acid (PAA), known in the literature as a good cation exchanger and proton electrolyte [18,19], is quite justified.

It is important to mention that the MF-4SK membranes, modified with polyantimonic acid nanoparticles, exhibited improved proton conductivity values compared to results for the original MF-4SK membranes [20]. However, the increase in conductivity of the composite was observed only within a limited temperature range of 60 °C.

In studies of other works, it was reported that the surface modification of PAA particles with potassium dihydrogen phosphate [21] leads to an increase in proton conductivity in a wider temperature range; however, the interfacial layer of resulting composite contains phosphoric acid, which is washed out of the membrane during the operation of the fuel cell.

Since PAA and compounds based on it are practically insoluble in water, this cannot lead to their washing from membranes during operation in various devices. From this point of view, for polymer composites based on Nafion, it seems promising to use particles with a modified surface containing additional atoms of polyantimonic acids to improve the affinity of the particles to the membrane.

In the present work, the results of the functionalization of the PAA particles surface with silicon oxide are presented and the structural and electrophysical properties of the obtained composite particles of "core-shell" structure are studied.

Experimental

The synthesis of composite particles with "core-shell" structure using PAA and SiO_2 involves combining equal amounts of PAA suspension and a 5 % solution of sodium silicate. At the same time, a suspension of PAA was obtained by a hydrolytic method in excess of distilled water, previously oxidized with nitric acid of antimony trichloride [22,23]. Modification of the surface of PAA particles with silicon oxide was carried out by holding the previously obtained PAA particles in concentrated hydrochloric acid for 3 days. The precipitate formed as a result of sedimentation of the suspension was repeatedly washed with distilled water until chloride ions were completely removed and dried in a muffle furnace at 110 °C for an hour.

The phase composition of the synthesized nanopowders was controlled by X-ray diffraction on a D8 Advance diffractometer (Bruker, Germany) in a given range of angles (2θ) from 10 to 70° using

an international database (ICDD JCPDS). The crystallographic parameters of the structure were refined by the Rietveld method in the PowderCell for Windows 2.4 software.

The surface morphology and elemental (chemical) composition of the obtained nanoparticles were studied using a JSM 7001F scanning electron microscope (JEOL, Japan) equipped with an INCAX-max 80 X-ray energy-dispersive (EDX) analysis system (Oxford Instruments, England).

The microstructure of surface-modified nanoparticles was studied using high-resolution transmission electron microscopy with a JEM-2100F (JEOL, Japan) microscope at an accelerating voltage of 100 kV. Custom software was used to obtain particle size distributions from transmission electron microscopy microphotographs. The Scope Photo program was utilized to study the distribution functions of nanoparticles.

The proton conductivity of the samples under study was measured by impedance spectroscopy on an Elins Z-1500J impedance meter ("Elins", Russia) in the frequency range from 100 Hz to 1 MHz in the temperature range from 100 to 200 °C. An impedance measurement cell capable of performing AC impedance measurements using a two-terminal connection circuit has been designed and manufactured. The measuring cell was a glass tube with graphite electrodes tightly fitted along the inner diameter of the tube. The cell was equipped with a system of pressure springs to ensure a constant contact area of the graphite electrodes with the sample under study. The sample, a fine powder, was placed in the cell by pouring the required amount of powder and pressing it under pressure springs. The cell filling coefficient with the sample under these conditions was 50 to 60 %.

Samples for measurements in the cell were cut out with a special device, which was a metal tube with a diameter similar to the internal diameter of the measuring cell, which made it possible to obtain disks with a thickness of 0.5 to 1 mm and a diameter of 3 mm with an accuracy of 0.02 mm. The cut disks were placed between graphite clamping electrodes.

The resistance of the samples was determined using the impedance hodographs from the high-frequency cut-off on the resistance axis. The values of conductivity σ were determined in accordance with the expression $\sigma = 4l/R_eS$, where l is the thickness of the sample, R_e is the resistance of the sample, and S is the area of the electrical contact.

Results and discussion

Figure 1 presents the results of X-ray diffraction studies of the initial composition of crystalline PAA (Figure 1a) and composite particles with "core-shell" structure obtained on the basis of PAA and silicon oxide (Figure 1b, c). According to the qualitative X-ray phase analysis data, the diffraction spectra of samples PAA@SiO_2 (Na-form) (Figure 1b) and PAA@SiO_2 (H-form) (Figure 1c) contain a strictly defined sequence of intense maxima (d_{hkl}), satisfactorily described by a quadratic form for crystals with a cubic type of crystal lattice symmetry, characteristic of the PAA sample.

In this case, the shape and half-width of the diffraction maxima recorded on the X-ray diffraction patterns do not change within the error of experimental measurements. The analysis of the extinction laws for reflections containing even and odd indices (*hkl*) showed that the symmetry of the lattice of the studied samples is preserved within the Fd-3m [22] space group. This allows us to conclude that as a result of ion-exchange processes occurring at the interphase boundary of PAA solid particles and sodium silicate solution, silicic acid is formed and adsorbed on the surface of the core of PAA particles, forming a shell, the thickness of which varies from 5 to 20 nm (Figure 2). Thus, the X-ray diffraction studies carried out in combination with high-resolution transmission electron microscopy data confirm the formation of nano-sized composite particles, the core of which has a pyrochlore-type structure, and the shell is an amorphous SiO_2.

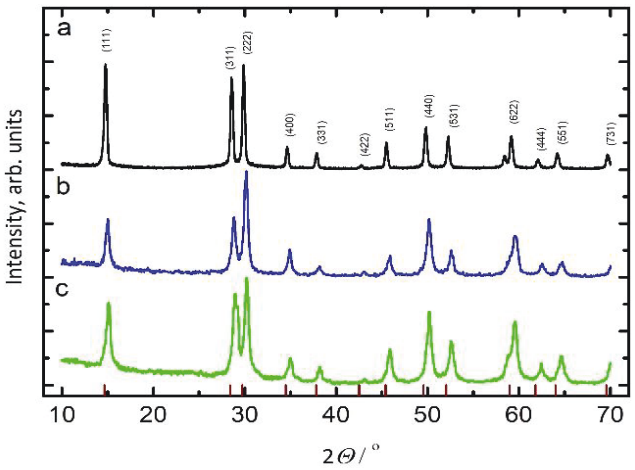

Figure 1. *X-ray diffraction patterns of PAA (a) and composite particles with "core-shell" structure based on PAA and silicon oxide: PAA@SiO_2 (Na-form) (b), PAA@SiO_2 (H-form) (c)*

An analysis of experimental data on the structural changes in the obtained composite nanoparticles using the Rietveld method made it possible to propose a model for the occupation of crystallographic positions by ions within Fd-3m space group (Table 1). According to this model, the framework of the structure is a three-dimensional network formed by vertex-jointed antimony-oxygen polyhedra of $[Sb(V)O_{6/2}]^-$gross composition of octahedral coordination [24] similar to PAA [18,19]. In this structure, Sb^{5+} and O^{2-} are statistically located in 16c and 48f positions, respectively, while Na^+ occupies 16d positions, and neutral water molecules can be located in nonequivalent 32e positions.

Table 1. *Model for the occupation of crystallographic positions by ions within sp. gr. Fd-3m for composite particles with "core-shell" structure based on PAA and silicon oxide*

Structural formula	Ion occupation of crystallographic positions				*a* /nm	wR_p / %
	16d	16c	48f	32e		
$NaSbO_3$	$14Na^+$ $2H_3O^+$	$16Sb^{5+}$	$40O^{2-}$	$16H_2O$	1.0276±0.0003	9.56
$HSbO_3$	$3Na^+$ $13H_3O^+$		$8OH^-$		1.0341±0.0003	9.30

a - crystal lattice parameter; wR_p - weighted profile value

As can be seen from Figure 2, the TEM photographs of the samples under study show a phase contrast of the images. Areas of dark contrast are PAA particles with a size less than 100 nm, consisting of several intergrown single crystals along [111], as evidenced by the presence of a network of parallel lines with interplanar distance d_{111} = 0.695 nm. In areas of light contrast, on the contrary, the absence of lines of atomic planes is observed, which indicates the presence of an amorphous phase of polysilicic acid on the surface of PAA particles - the so-called “shell” with a thickness of up to 20 nm.

The analysis of the particle size distribution function showed that the largest number of PAA nanoparticles are characterized by sizes varying in the range from 60 to 80 nm (Figure 3). At the same time, the composite sample contains smaller particles with sizes up to 30 nm (Figure 3).

After washing the particles from sodium ions, energy-dispersive analysis was carried out to control the elemental composition of nanostructured samples. The results showed a uniform distribution of antimony, silicon, and oxygen ions over the entire surface of the sample under study, as shown in Figure 4.

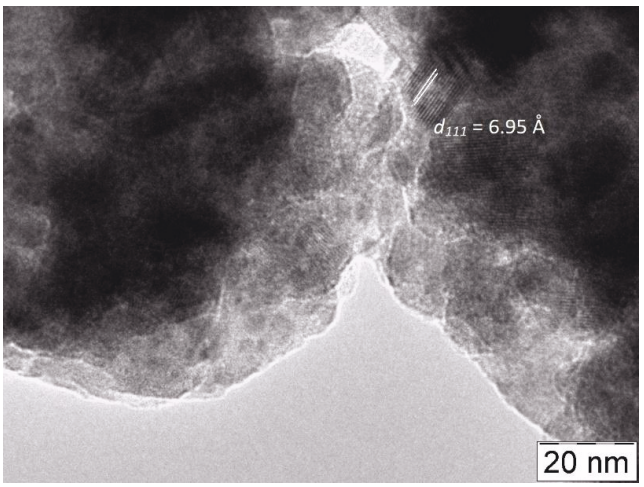

Figure 2. *TEM image of PAA@SiO_2 (Na-form) composite nanoparticles*

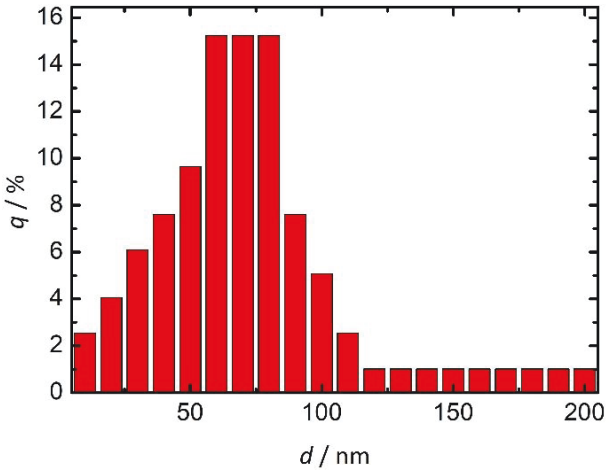

Figure 3. *Histogram of particle size distribution for PAA nanoparticles where q is the fraction of particles of a given diameter; d is the particle size*

The results of the detailed mapping of the elements contained in the composites under study (Table 2) are presented in Figure 5 and confirm the presence of an amorphous phase of polysilicic acid on the surface of PAA nanoparticles.

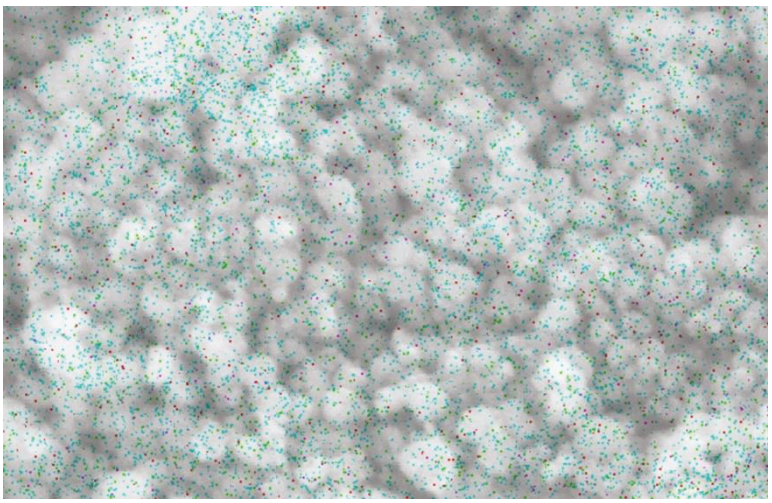

Figure 4. *Multilayer EDS map of PAA@SiO_2 (H-form) composite nanoparticles*

Table 2. *Elemental composition of the composite particles with "core-shell" structure based on PAA and SiO_2*

Composite nanoparticles	Content, at.%			
	Sb	O	Si	Na
PAA@SiO_2 (H-form)	53.54	35.77	4.51	6.18
PAA@SiO_2 (Na-form)	42.12	37.41	4.17	16.30

On electron microscopic images of nanostructured composites (Figure 6, left), at a magnification of 10000x, a uniform contrast is observed over the entire area of the resulting image. The diameter of the particles is characterized by similar values, not exceeding 100 nm. At a higher magnification, 30000x (Figure 6, right), it can be seen that large particles are aggregates about 100 nm in size, consisting of several smaller particles, the size of which varies in the range from 20 to 30 nm.

It should be noted that the particle cores and their shells in the nanocomposite structure (Figure 2) are separated from each other by a clear contrasting boundary resembling the boundary between phases, while in the PAA structure, the boundary between individual particles is more diffuse [25].

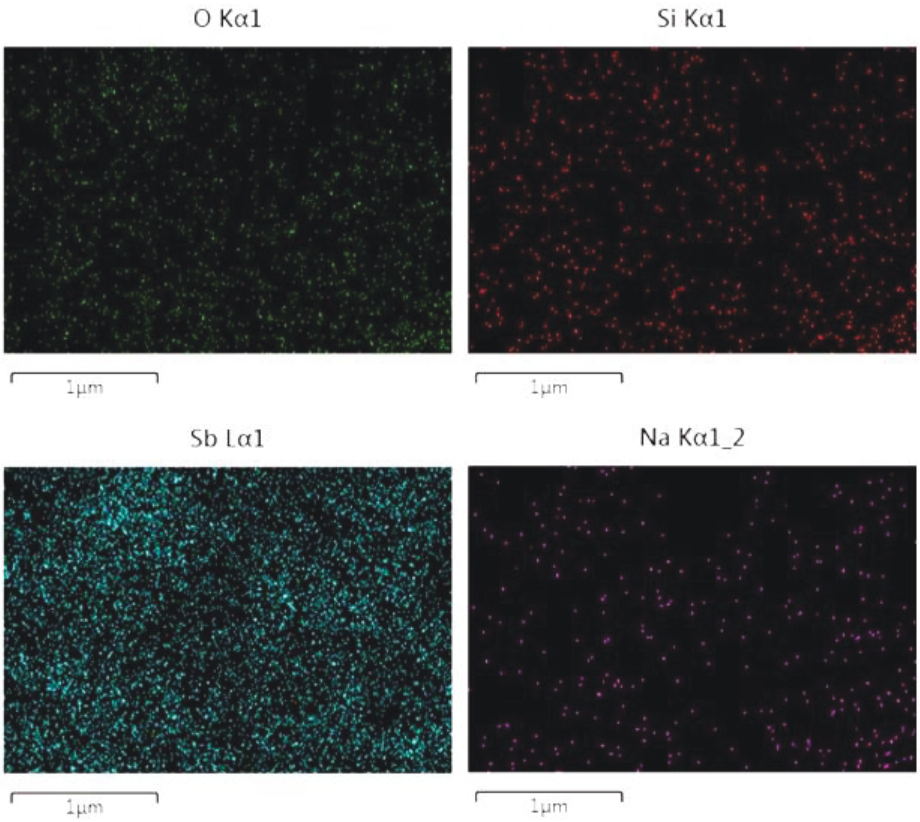

Figure 5. *Mapping of distribution of chemical elements of PAA@SiO_2 (H-form) composite particles with "core-shell" structure*

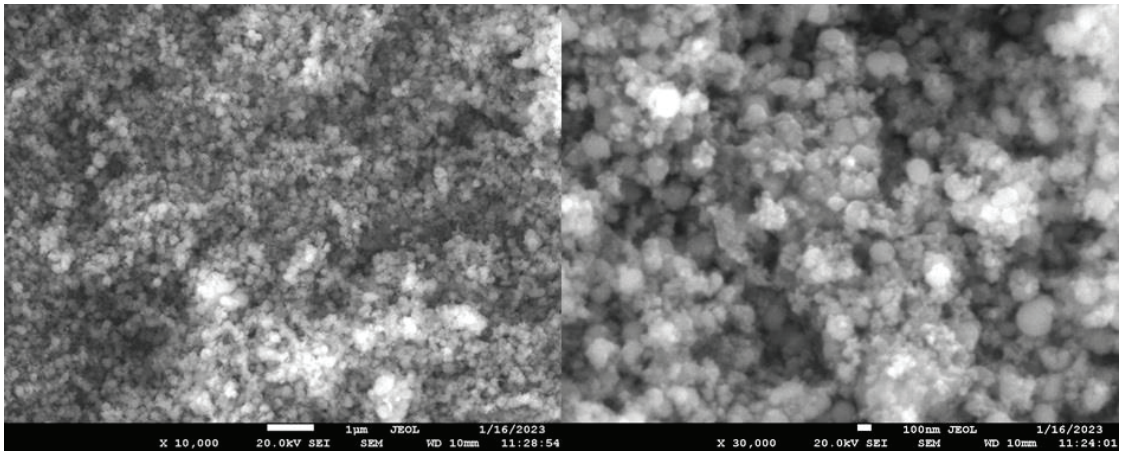

Figure 6. *Electron microscopic images of PAA@SiO_2 (Na-form) composite nanoparticles*

The measurements of the electrophysical properties for the studied nanoscale systems on alternating current allowed to determine the frequency dependences for the real and imaginary components of the complex impedance and to determine the equivalent circuits for composites with "core-shell" structure based on PAA and SiO_2. Figure 7 shows the impedance hodographs plotted in the Nyquist coordinates $Z''(f)$ and $Z'(f)$ at different temperatures. As can be seen, the obtained impedance hodographs of PAA@SiO_2 (H-form) sample are an arc of a semicircle that emerges from the origin in the high-frequency region and a part of the semicircle, transforming into a "spur" in the region of medium and low frequencies of the electric field. With increasing temperature, the radius of the semicircular arc decreases, which indicates a decrease in the resistance. The measured spectral characteristics of the complex impedance were found to be qualitatively similar to those reported by the authors of [25], who studied the electrical response of PAA-based polycrystalline materials.

The construction of the impedance hodograph facilitates the search for a suitable equivalent circuit, the impedance of which should approximate the experimentally measured impedance spectrum of the sample in all studied frequency ranges.

Thus, for PAA@SiO_2 (Na-form) nanocomposite, the equivalent circuit is a link (Figure 8a) in which the capacitance of the intergranular space C_1 and the resistance of the test sample R_1 (Table 3) are connected in parallel. This link is designed to approximate a small semicircular arc in the high-frequency region. The electrophysical processes occurring in the high-frequency region in a sample of the composition PAA@SiO_2 (H-form) can be described by an equivalent circuit with a similar form (Figure 8a).

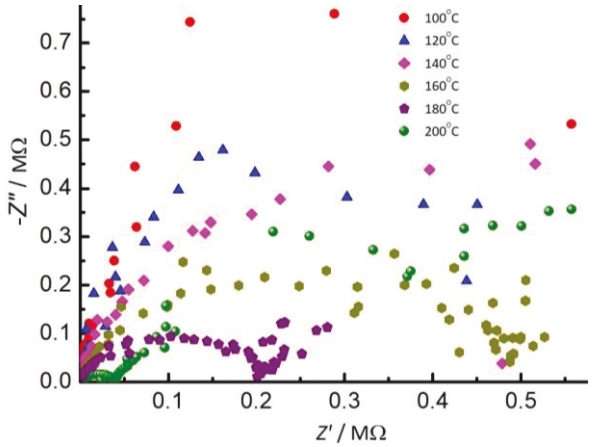

Figure 7. *Nyquist plots of the PAA@SiO_2 (H-form) nanocomposite*

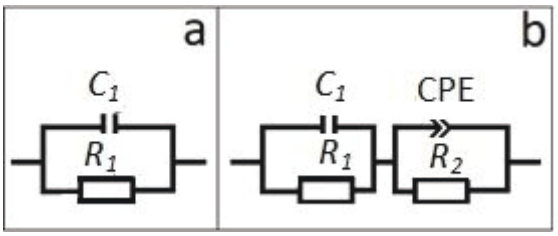

Figure 8. *Equivalent circuit schemes for composites with "core-shell" structure based on PAA and SiO_2 of Na-form (a); H-form (b)*

Table 3. *Values of equivalent circuit elements R_1 and C_1 for composite "core-shell" particles based on PAA and SiO_2 (Na- and H-forms)*

T / °C	PAA@SiO_2 (Na-form)			PAA@SiO_2 (H-form)		
	R_1 / MΩ	C_1 / pF	σ / μS m^{-1}	R_1 / MΩ	C_1 / pF	σ / μS m^{-1}
100	$1.00 \cdot 10^{14}$	3.44	$2.06 \cdot 10^{-13}$	1.02	12.5	23.1
110	$1.00 \cdot 10^{14}$	3.34	$2.06 \cdot 10^{-13}$	0.8	16.2	28.8
120	$1.00 \cdot 10^{14}$	3.40	$2.06 \cdot 10^{-13}$	2.10	6.91	11.2
130	$1.25 \cdot 10^{14}$	3.40	$1.65 \cdot 10^{-13}$	1.44	6.93	16.4
140	$1.00 \cdot 10^{14}$	3.34	$2.06 \cdot 10^{-13}$	1.03	6.57	22.8
150	49.5	3.50	0.417	0.734	6.50	32.1
160	37.1	3.59	0.556	0.409	6.62	57.7
170	10.3	3.31	2.00	0.255	7.08	92.7
180	9.55	3.81	2.16	0.168	6.81	140
190	3.74	6.06	5.51	0.120	6.40	197
200	3.26	6.36	6.32	0.0355	6.92	665

When describing the physical processes in the system under study in the low-frequency range of the electric field, the elements of the equivalent circuit differ from each other. In particular, an extra link is added in series with C_1 and R_1 (Table 3), which are connected in parallel. This link contains a parallel circuit connecting the constant phase shift element - CPE and R_2 (Figure 8b). The second link of the scheme models the region in which the near-electrode physicochemical processes of adsorption-desorption and the formation of a double electric layer can occur. Further, when analyzing the experimentally obtained results of the impedance spectra of the studied composite systems with the "core-shell" structure, such processes will not be considered.

In accordance with the data on proton conductivity σ (Table 3), within the limits of measurement error, Arrhenius-type dependencies $\log \sigma = f(1/T)$ were obtained (Figure 9) and for the studied temperature range the conductivity activation energy E_a of the nanocomposite PSA@SiO_2 (H-form) composition was determined to be 50 kJ mol^{-1} or 0.52 eV.

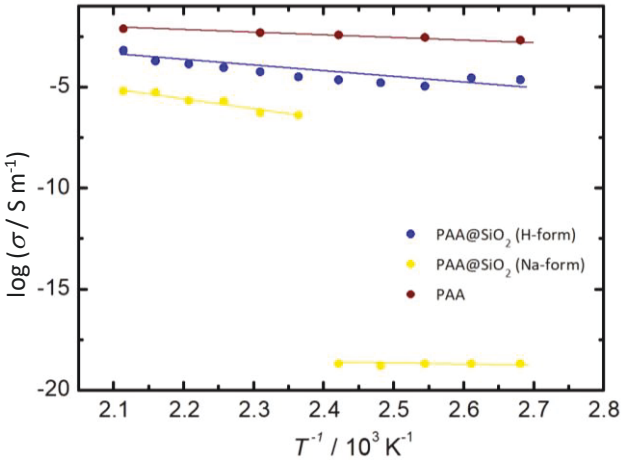

Figure 9. *Reciprocal temperature dependencies of the conductivity for PAA sample and composites with "core-shell" structure based on PAA and SiO_2 (H- and Na-forms)*

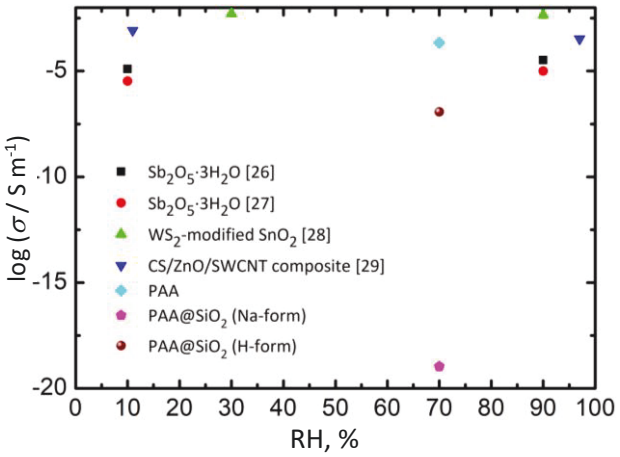

Figure 10. *Relative humidity (RH) of the environment dependencies of the conductivity for PAA sample and composites with "core-shell" structure based on PAA and SiO_2 (H- and Na-forms) and various compositions at room temperature*

Figure 10 presents the results of a comparison of the conductivity calculated values for the studied samples of various compositions at room temperature depending on the ambient humidity. As can be seen, the calculated values of the conductivity of the obtained composites are in good agreement with the data of other works [26-30].

Conclusions

This article considered the possibility of functionalizing the surface of PAA particles with silicon oxide. The result of the work is the obtaining of composite particles with "core-shell" structure, where the core is polycrystalline PAA particles, and the shell is a layer of amorphous silicon oxide up to 20 nm thick. The performed X-ray diffraction studies have shown that, upon ion exchange, the symmetry of the crystal lattice of the synthesized nanosized composite particles is preserved within sp. gr. Fd-3m.

The refined crystallographic parameters of the resulting composite nanoparticles using the Rietveld method allowed us to propose a model of ion occupation in a pyrochlore-type structure,

according to which the framework of the structure is formed by Sb^{5+} and O^{2-}, statistically located in the 16c and 48f positions, while Na^+ and H_2O molecules are distributed over the 16d and 32e positions, respectively.

Based on experimental impedance spectroscopy data of the studied composites with "core-shell" structure based on PAA and SiO_2, the resulting impedance hodographs were analyzed and equivalent circuits were determined. For a nanocomposite of PAA@SiO_2 (H-form) composition, a linear dependence of the logarithm of the specific conductivity on the inverse temperature. The activation energy of conductivity E_a was determined in the temperature range under study, the value of which was 0.52 eV. The resulting nanocomposite satisfies the requirement for the conductivity of materials in the region of 333 to 453 K for their use as proton-conducting membranes in low-temperature fuel cells and humidity sensors.

Acknowledgment: *This work has been supported by the grants the Russian Science Foundation, RSF 23-23-00140.*

References

[1] E. Yu. Safronova, A. B. Yaroslavtsev. Prospects of practical application of hybrid membranes, *Petroleum Chemistry* **56** (2016) 281-293. https://doi.org/10.1134/S0965544116040083

[2] S. S. Ivanchev, S. V. Myakin. Polymer membranes for fuel cells: manufacture, structure, modification, properties, *Russian Chemical Reviews* **79(2)** (2010) 101-117. https://doi.org/10.1070/RC2010v079n02ABEH004070

[3] H. Strathmann, A. Grabowski, G. Eigenberger. Ion-Exchange Membranes in the Chemical Process Industry, *Industrial & Engineering Chemistry Research* **52** (2013) 10364. https://doi.org/10.1021/IE4002102

[4] S. A. Novikova, G. Yu. Yurkov, A. B. Yaroslavtsev. Synthesis and transport properties of membrane materials with metal nanoparticles incorporated, *Mendeleev Communications* **20(2)** (2010) 89-91. https://doi.org/10.1016/j.mencom.2010.03.008

[5] I. A. Stenina, A. S. Shalimov, A. B. Yaroslavtsev. Ion transfer in hybrid inorganic/organic membranes, *Polymers for Advanced Technologies* **6** (2009) 566-570. https://doi.org/10.1002/pat.1384

[6] E. Yu. Safronova, A. B. Yaroslavtsev. Nafion-type membranes doped with silica nanoparticles with modified surface, *Solid State Ionics* **221** (2012) 6-10. https://doi.org/10.1016/j.ssi.2012.05.030

[7] V. Di Noto, N. Boaretto, E. Negro, G. Pace. New inorganic–organic proton conducting membranes based on Nafion and hydrophobic fluoroalkylated silica nanoparticles, *Journal of Power Sources* **195(23)** (2010) 7734-7742. https://doi.org/10.1016/j.jpowsour.2009.10.028

[8] E. Y. Safronova, I. A. Stenina, A. B. Yaroslavtsev. Synthesis and characterization of MF-4SK+SiO_2 hybrid membranes modified with tungstophosphoric heteropolyacid, *Russian Journal of Inorganic Chemistry* **55(1)** (2010) 13-17. https://doi.org/10.1134/S0036023610010031

[9] K. Oh, O. Kwon, B. Son, D. H. Lee, S. Shanmugam. Nafion-sulfonated silica composite membrane for proton exchange membrane fuel cells under operating low humidity condition, *Journal of Membrane Science* **583** (2019) 103-109. https://doi.org/10.1016/j.memsci.2019.04.031

[10] E. Gerasimova, E. Safronova, A. Ukshe, Y. Dobrovolsky, A. Yaroslavtsev. Electrocatalytic and transport properties of hybrid Nafion membranes doped with silica and cesium acid salt of phosphotungstic acid in hydrogen fuel cells, *Chemical Engineering Journal* **305** (2016) 121-128. https://doi.org/10.1016/j.cej.2015.11.079

[11] G. Xu, Z. Wei, S. Li, J. Li, Z. Yang, S. A. Grigoriev. In-situ sulfonation of targeted silica-filled Nafion for high-temperature PEM fuel cell application, *International Journal of Hydrogen Energy* **44(56)** (2019) 29711-29716. https://doi.org/10.1016/j.ijhydene.2019.02.037

[12] D. Cozzi, C. de Bonis, A. D'Epifanio, B. Mecheri, A. C. Tavares, S. Licoccia. Organically functionalized titanium oxide/Nafion composite proton exchange membranes for fuel cells applications, *Journal of Power Sources* **248** (2014) 1127-1132. https://doi.org/10.1016/j.jpowsour.2013.10.070

[13] D. V. Golubenko, R. R. Shaydullin, A. B. Yaroslavtsev. Improving the conductivity and permselectivity of ion-exchange membranes by introduction of inorganic oxide nanoparticles: impact of acid–base properties, *Colloid and Polymer Science* **297** (2019) 741-748. https://doi.org/10.1007/s00396-019-04499-1

[14] P. A. Yurova, V. R. Malakhova, E. V. Gerasimova, I. A. Stenina, A. B. Yaroslavtsev. Nafion/Surface Modified Ceria Hybrid Membranes for Fuel Cell Application, *Polymers* **13(15)** (2021) 2513. https://doi.org/10.3390/polym13152513

[15] E. Bakangura, L. Wu, L. Ge, Z. Yang, T. Xu. Mixed matrix proton exchange membranes for fuel cells: State of the art and perspectives, *Progress in Polymer Science* **57** (2016) 103-152. https://doi.org/10.1016/j.progpolymsci.2015.11.004

[16] C. Y. Wong, W. Y. Wong, K. Ramya, M. Khalid, K. S. Loh, W. R. W. Daud, A. A. H. Kadhum. Additives in proton exchange membranes for low- and high-temperature fuel cell applications: A review, *International Journal of Hydrogen Energy* **44** (2019) 6116-6135. https://doi.org/10.1016/j.ijhydene.2019.01.084

[17] D. J. Kim, M. J. Jo, S. Y. Nam. A review of polymer–nanocomposite electrolyte membranes for fuel cell application, *Journal of Industrial and Engineering Chemistry* **21** (2015) 36-52. https://doi.org/10.1016/j.jiec.2014.04.030

[18] F. A. Belinskaya, E. A. Militsina. Inorganic Ion-exchange Materials Based on Insoluble Antimony(V) Compounds, *Russian Chemical Reviews* **49** (1980) 933-952. https://doi.org/10.1070/RC1980v049n10ABEH002518

[19] V. P. Balykin, V. A. Burmistrov, O. A. Mezhenina. Structure and ion exchange properties of crystalline polyantimonic acid, *Bulletin of the South Ural State University, series "Chemistry"* **8(13)** (2012) 43-48. https://vestnik.susu.ru/chemistry/article/view/1899 (in Russian)

[20] F. A. Yaroshenko, V. A. Burmistrov. Synthesis of Hybrid Materials Based on MF-4SK Perfluorinated Sulfonated Cation-Exchange Membranes Modified with Polyantimonic Acid and Characterization of Their Proton Conductivity, *Petroleum Chemistry* **58(9)** (2018) 770-773. https://doi.org/10.1134/S0965544118090116

[21] D. A. Zakharyevich, A. S. Neustroev. Proton Conduction Through Interface Phase of CPAA/KDP Composites, *MRS Proceedings* **1256** (2010) 1642. https://doi.org/10.1557/PROC-1256-N16-42

[22] L. Yu. Kovalenko, V. A. Burmistrov, Yu. A. Lupitskaya, F. A. Yaroshenko, E. M. Filonenko, E. A. Bulaeva. Ion exchange of H^+/Na^+ in polyantimonic acid, doped with vanadium ions, *Pure and Applied Chemistry* **92(3)** (2020) 505-514. https://doi.org/10.3390/app112411877

[23] T. Yu, Y. Shen, H. Zhang, S. Xu, H. Cao, G. Zheng. Efficient Removal of Bismuth with Supersoluble Amorphous Antimony Acids: An Insight into Synthesis Mechanism and Sb(V)-Bi(III) Interaction Behaviors, *Chemical Engineering Journal* ***420*** (2021) 127617. https://doi.org/10.1016/j.cej.2020.127617

[24] Yu. A. Lupitskaya, F. A. Yaroshenko, E. M. Filonenko, O. A. Firsova. Structure and ion-exchange properties of tungsten-antimony crystalline acid and its substituted forms, *Chelyabinsk Physical and Mathematical Journal* **6(4)** (2021) 485-496. https://doi.org/10.47475/2500-0101-2021-16408

[25] O. Y. Kurapova, P. M. Faia, A. A. Zaripov, V. V. Pazheltsev, A. A. Glukharev, V. G Konakov. Electrochemical Characterization of Novel Polyantimonic-Acid-Based Proton Conductors for Low- and Intermediate-Temperature Fuel Cells, *Applied Sciences* **11** (2021) 11877. https://doi.org/10.3390/app112411877

[26] S. Mendes, O. Kurapova, P. Faia. Enhancing Polyantimonic-Based Materials Moisture Response with Binder Content Tuning, *Chemosensors* **11** (2023) 423. https://doi.org/10.3390/chemosensors11080423

[27] S. Mendes, O. Kurapova, P. Faia, V. Pazheltsev, A. Zaripov, V. Konakov. Polyantimonic Acid-Based Materials Evaluated as Moisture Sensors at Ambient Temperature, *Journal of Solid State Electrochemistry* **27** (2023) 611-625. https://doi.org/10.1007/s10008-022-05352-2

[28] Y. Chen, Y. Pei, Z. Jiang, Z. Shi, J. Xu, D. Wu, T. Xu, Y. Tian, X. Wang, X. Li. Humidity Sensing Properties of the Hydrothermally Synthesized WS_2-Modified SnO_2 Hybrid Nanocomposite, *Applied Surface Science* **447** (2018) 325-330. https://doi.org/10.1016/j.apsusc.2018.03.154

[29] H. Dai, N. Feng, J. Li, J. Zhang, W. Li. Chemiresistive humidity sensor based on chitosan/zinc oxide/single-walled carbon nanotube composite film, *Sensors and Actuators B* **283** (2020) 786-792. https://doi.org/10.1016/j.snb.2018.12.056

[30] O. Y. Kurapova, A. A. Zaripov, V. V. Pazheltsev, A. G. Glukharev, V. G. Konakov. Bulk solid state polyantimonic acid based proton conducting membranes. *Novye Ogneupory (New Refractories)* **2** (2022) 45-50. https://newogneup.elpub.ru/jour/article/view/1731 (in Russian)